Does the clinical phenotype of mucolipidosis-IIIγ differ from its αβ counterpart?: supporting facts in a cohort of 18 patients

Sheela Nampoothiri[a], Nursel H. Elcioglu[h], Suleyman S. Koca[i], Dhanya Yesodharan[a], Chandrababu KK[b], Vinod Krishnan V[b], Meenakshi Bhat[f], Mohandas Nair K[e], Natasha Radhakrishnan[c], Mahesh Kappanayil[d], Jayesh J. Sheth[g], Sandra Alves[j], Francisca Coutinho[j], Michael J. Friez[k], Richard M. Pauli[l], Sheila Unger[m], Andrea Superti-Furga[m], Jules G. Leroy[k] and Sara S. Cathey[k]

Mucolipidosis-IIIγ (ML-IIIγ) is a recessively inherited slowly progressive skeletal dysplasia caused by mutations in *GNPTG*. We report the genetic and clinical findings in the largest cohort with ML-IIIγ so far: 18 affected individuals from 12 families including 12 patients from India, five from Turkey, and one from the USA. With consanguinity confirmed in eight of 12 families, molecular characterization showed that all affected patients had homozygous pathogenic *GNPTG* genotypes, underscoring the rarity of the disorder. Unlike ML-IIIαβ, which present with a broader spectrum of severity, the ML-III γ phenotype is milder, with onset in early school age, but nonetheless thus far considered phenotypically not differentiable from ML-IIIαβ. Evaluation of this cohort has yielded phenotypic findings including hypertrophy of the forearms and restricted supination as clues for ML-IIIγ, facilitating an earlier correct choice of genotype screening. Early identification of this disorder may help in offering a timely intervention for the relief of carpal tunnel syndrome, monitoring and surgery for cardiac valve involvement, and evaluation of the need for joint replacement. As this condition may be confused with rheumatoid arthritis, confirmation of diagnosis will prevent inappropriate use of immunosuppressants and disease-modifying agents. *Clin Dysmorphol* 28:7–16 Copyright © 2018 Wolters Kluwer Health, Inc. All rights reserved.

Clinical Dysmorphology 2019, **28:**7–16

Keywords: carpal tunnel syndrome, clawing of fingers, genu valgum, *GNPTG*, hypertrophy of forearm, mucolipidosis-IIIαβ, mucolipidosis IIIγ

Departments of [a]Pediatric Genetics, [b]Orthopedics, [c]Ophthalmology, [d]Pediatric Cardiology, Amrita Institute of Medical Sciences and Research Center, Kerala, [e]Department of Pediatrics, Government Medical College, Kozhikode, [f]Department of Clinical Genetics, Centre for Human Genetics, Bangalore, [g]Department of Biochemical and Molecular Genetics, FRIGE's Institute of Human Genetics, Ahmedabad, India, [h]Department of Pediatric Genetics, Marmara University Faculty of Medicine, Istanbul, [i]Department of Rheumatology, Firat University Faculty of Medicine, Elazig, Turkey, [j]Research and Development Unit, Human Genetics Department, National Health Institute Dr. Ricardo Jorge, Porto, Portugal, [k]Greenwood Genetic Center, Greenwood, South Carolina, [l]University of Wisconsin School of Medicine and Public Health, Madison, Wisconsin, USA and [m]Division of Genetic Medicine, Lausanne University Hospital, University of Lausanne, Lausanne, Switzerland

Correspondence to Sheela Nampoothiri, DCH, Dip NB, MSc, Department of Pediatric Genetics, Amrita Institute of Medical Sciences and Research Center, Cochin 682041, Kerala, India
Tel: +91 484 285 1234; fax: +91 484 280 2020; e-mail: sheeladr@gmail.com

Received 7 August 2018 **Accepted** 6 September 2018

Introduction

Mucolipidosis-IIIγ (ML-IIIγ) (MIM 252605) is a rare, slowly progressive inborn error of connective tissue metabolism with skeletal dysplasia as its most overt and ultimately most morbid phenotypic feature. The mode of inheritance is autosomal recessive. It is caused by biallelic mutations in *GNPTG* that encodes the γ subunit of UDP-*N*-acetylglucosamine lysosomal enzyme *N*-acetylglucosamine-1-phosphotransferase (GlcNAc-phosphotransferase, GNPTG) (EC 2.7.8.17), a hexameric protein complex composed of two copies each of the α, β, and γ polypeptides. The enzyme catalyzes the first step in the biosynthesis of the mannose-6-phosphate (M6P) recognition marker in the glycan part of most lysosomal hydrolases (Hasilik and Von Figura, 1981; Reitman and Kornfeld, 1981). This carbohydrate marker is crucial for binding of the nascent acidic lysosomal glycoproteins to M6P receptors in the Golgi apparatus. The enzyme–receptor complexes are thus targeted to the lysosomal cell compartment, where they dissociate because of the ambient acid pH, allowing the receptors to recycle to the Golgi apparatus for more rounds of transport (Hasilik and Von Figura, 1986; Kornfeld, 1992; Pohl *et al*., 2010). Without the M6P recognition marker, nascent lysosomal hydrolases are not targeted to lysosomes in connective tissue cells. Instead, they are lost into the interstitial spaces. Intralysosomal deficiency of lysosomal hydrolases leads to the accumulation of heterogeneous undegraded macrocompounds in the organelles that appear microscopically as granular cytoplasmic inclusion bodies, hence the term 'inclusion cells' ('I cells') (Leroy *et al*., 1969; Taylor *et al*., 1973; Leroy, 2011). The phenomenon is best visible by phase-contrast microscope observation in cultured mutant fibroblasts of ML-II and ML-IIIαβ patients.

DOI: 10.1097/MCD.0000000000000249

ML-IIIγ fibroblasts also have this remarkable tissue culture phenotype. The lack of proper targeting results in loss of the structurally abnormal enzymes into the extracellular space. Consequently, enhanced lysosomal hydrolase activity is measurable not only in the in-vitro culture media but also in the patient's plasma. Since genotyping has become available, the histological sign no longer plays a major role in the objective diagnosis of any of the *N*-acetylglucosamine-1-phosphotransferase (GNPT) type mucolipidoses (Raas-Rothschild *et al.*, 2000; Cathey *et al.*, 2010). The α and β subunits in the enzyme complex are encoded by *GNPTAB* on chromosome 12q23.2. Proteolytic cleavage by site-1 protease (Marschner *et al.*, 2011) at the Lys 928-Asp 929 peptide bond yields the mature α and β polypeptides that form the Golgi membrane-bound phosphotransferase. Normal catalytic action requires the recruitment of two soluble γ chains for effective substrate recognition and phosphorylation of some acid hydrolases. Homozygous or compound heterozygous pathogenic *GNPTAB* mutations cause either the severe ML-II or ML-IIIαβ, the latter dependent on the amount of residual GNPT activity (Kudo *et al.*, 2006; Cathey *et al.*, 2010). ML-IIIγ, a disorder nonallelic to ML-IIIαβ, is considered to be clinically hardly differentiable from ML-IIIαβ (Raas-Rothschild *et al.*, 2000, 2004; Kudo *et al.*, 2006; Encarnação *et al.*, 2009; Persichetti *et al.*, 2009).

The study of this largest cohort of ML-IIIγ patients offers the opportunity to improve our knowledge of the phenotype. We observe some unique phenotypic features in ML-IIIγ that challenge the current idea of phenotypic identity with ML-IIIαβ. As 12 of 18 patients in this cohort are from India, ML-IIIγ is likely to have a pan-ethnic distribution contrary to the previous reports mainly from the Mediterranean region.

Patients and methods

The diagnosis of ML-IIIγ was made on the basis of clinical, radiological, and biochemical studies and *GNPTG* mutation screening in 18 patients from 12 families. The clinical evaluation was the result of the combined efforts and mutual consultations by six clinical geneticists and one rheumatologist. Dysostosis multiplex was recognized in 17 of 18 patients by studying at least one set of films covering the entire skeleton. Echocardiographic and ophthalmologic examinations have yielded the degree of multisystemic involvement. Metabolic support for the diagnosis of ML-III was provided by the assay of selected acid lysosomal hydrolases in the plasma of 16 of 18 patients and revealed at least a 10-fold increase.

Sequence analysis of the coding regions and flanking intron sequences of *GNPTG* was carried out in DNA isolated from blood samples. Individual exons were amplified with custom-designed primers (available by request). After gel electrophoresis confirmed successful amplification, the amplicons were purified by QIA quick columns or plates (Qiagen, Germantown, Maryland, USA). Sequencing was performed using a standard Big Dye protocol (Thermo Fisher, Waltham, Massachusetts, USA), followed by purification using DyeEx columns or plates (Qiagen). Products were run on an ABI3730 DNA Sequencer in the Molecular Diagnostic Laboratory at the Greenwood Genetic Center (Greenwood, South Carolina, USA). Finished sequence data were compared with normal controls and the published *GNPTAB* text sequence using Sequencer software (Gene Codes Corporation, Ann Arbor, Michigan, USA).

Results

Clinical spectrum

The cohort comprised 12 female and six male patients from 12 families including 10 children ranging in age from 5 to 12 years and eight adults aged $18^1/_2$ to 37 years.

The anthropometric measurements and clinical features of all 18 patients are presented in Table 1. Parental consanguinity was confirmed in eight of 12 families. The average age of onset in this cohort was estimated to be around 5 years. The age range at first symptom was wide and overlapped with that known in ML-IIIαβ. Establishing the true age of onset in these chronic disorders remains a challenging task, whereas in ML-II, features are present at or even before birth (Saul *et al.*, 2005).

The most common presenting symptom in our cohort was stiffness in multiple joints: clawing of the fingers (18/18) (Fig. 1a and b), wrist (18/18), hip (10/18), and shoulder (12/18) (Fig. 2a). Widening of the wrist joint was observed in 15 of 18 (Fig. 1c and d). This feature, along with stiffness of the fingers, had initially led to the clinical impression of rheumatoid arthritis in six of 18 patients (Fig. 1e). Early signs of coarsening of facial features were apparent in some children (Fig. 2f and g). Slit-lamp evaluation in the children showed mild corneal clouding in eight of 12 patients (Fig. 2c). Stature was below the third percentile in three patients, the 3rd to 5th percentile in 10 patients, the 10th to 25th percentile in two patients, and the 25th to 50th percentile in two patients. Height measurements were unavailable for patient 17. The mean adult height was 146 cm (range: 135–159 cm). Weight and occipitofrontal circumference were proportionate to stature.

Attention was focused on the differences from the ML-IIIαβ phenotype. Prominent among them were inability of forearm supination (16/18) as early as 7 years (Fig. 2b); hypertrophy of the forearms in seven of 18 patients (Figs 1c and d and 2b); woody skin texture (16/18) (Fig. 1g) initially manifesting on the dorsal aspect of the hands and later on involving the facial skin; and carpal tunnel syndrome (18/18) by adolescence. The carpal tunnel syndrome was already apparent at age 5 years in patient 4 and required surgical release in seven of 18 patients. Slowly progressive wasting of thenar and hypothenar eminences was observed in 13 of 18 patients (Fig. 1f and h).

Table 1 Anthropometric measurements and clinical features of 18 patients

Families	1		2		3	4	5	6		7	8		9		10		11	12
Patient number	1	2	3	4	5	6	7	8	9	10	11	12	13	14	15	16	17	18
Age (years)	20	$18^{1}/_{2}$	10	5	12	7	9	$8^{7}/_{12}$	$5^{8}/_{12}$	$10^{5}/_{12}$	$7^{4}/_{12}$	$7^{3}/_{4}$	26	20	37	26	31	19
Sex	M	M	M	F	F	M	F	F	M	F	M	F	F	F	F	F	F	F
Nationality	I	I	I	I	I	I	I	I	I	I	I	I	T	T	T	T	T	C
Consanguinity	+	+	−	−	−	+	−	+	+	+	+	+	+	+	+	+	+	−
Affected sib	+	+	+	+	−	−	−	+	+	+	+	−	+	+	+	+	−	−
Height (cm, centile)	159 (< 5th)	147 (< 5th)	121 (< 5th)	103 (10–25th)	129 (< 3rd)	110 (< 5th)	114 (< 5th)	129 (25–50)	108 (10–25)	114 (< 3rd)	100 (< 3rd)	125 (25–50)	140 (< 5th)	135 (< 5th)	146 (< 5th)	152 (< 5th)	NA	146 (< 5th)
Weight (kg, centile)	39 (< 5th)	36 (< 5th)	22 (< 5th)	15 (10th)	23 (< 3rd)	15 (< 5th)	19 (< 5th)	27 (50–75)	15 (3–10)	20 (< 3rd)	14 (< 3rd)	25 (50th)	40 (< 5th)	35 (< 5th)	50 (10–25th)	46 (< 5th)	NA	53 (25th)
HC (cm, centile)	52	52.5 (< 3rd)	49.5 (< 3rd)	47.5 (< 3rd)	51.5 (10th)	48 (< 3rd)	49 (< 3rd)	50.5 (25–50)	49 (3–10)	50 (< 3rd)	49.5 (3rd)	49 (3rd)	55	51	53	52	NA	55 (50th)
Coarse face	+	+	+	−	+	+	+	+	−	+	−	−	+	+	+	+	+	+
Corneal clouding	+	+	−	−	+	−	+	+	+	+	−	+	ND	ND	ND	ND	ND	−
Woody skin	+	+	++	+	++	+	+	+	+	+	−	−	+	+	+	++	+	+
Restricted mobility																		
Fingers	+	+	+	+	+	+	+	+	+	+	+	+	+	+	+	+	+	+
Shoulder	+	+	+	−	+	+	+	+	+	+	−	+	−	−	−	−	+	+
Elbow	+	+	+	−	+	+	+	+	+	+	+	+	−	−	−	−	−	+
Wrist	+	+	+	+	+	+	+	+	+	+	+	+	+	+	+	+	+	+
Hip	+	+	−	−	−	−	−	−	−	+	+	−	++	+	++	+	+	+
Knee	+	+	−	−	−	−	+	+	−	−	−	−	−	−	−	+	+	+
Difficulty to squat	+	+	+	+	+	+	+	+	−	+	+ +	+	ND	ND	ND	ND	ND	-
Hip pain	−	−	−	−	−	−	−	−	−	−	−	+	+	+	+	++	+	−
Ankle contracture	+	+	−	−	−	−	+	+	−	−	−	+	+	+	−	−	+	+
Genu valgum	−	+	++	+	+++	+	++	++	+++	+	+	++	+	+	−	−	−	−
Wrist widening	+	++	++	+	++	++	+	+	+	++	++	+	−	−	+	+	−	+
Hypertrophy of forearm	+	++	+++	−	+++	+++	+	−	−	+	−	−	−	−	−	−	−	−
Wasting of palmar muscles	++	+	+	−	++	−	++	++	−	++	NA	+	++	++	+++	+++	++	NA
Carpal tunnel syndrome	+	+	+	+	+	+	+	++	+	+	+	+	+	+	+	+	+	+
Scoliosis	−	+	−	−	−	−	−	+	−	−	−	−	+	+	+	+	−	−
Coxa valga	+, 148°	+, 142°	+, 151°	+, 148°	+, 146°	+, 147°	+, 148°	−, 130°	+, 147°	+, 152°	+, 146°	+, 146°	NA	NA	NA	+, 142°	−, 130°	+, 144°

C, Caucasian; HC, head circumference; I, Indian; LD, learning disability; N, normal; NA, not available; ND, not done; SD, supination defect; T, Turkish.

Fig. 1

(a) Early clawing in P4 at 5 years. (b) Advanced clawing with atrophy of thenar and hypothenar muscles and restriction of supination in P3 at 10 years. (c) (d) Hypertrophy of forearm with widening of both wrists in P3 at 10 years and P5 at 12 years. (e) Nodular swelling on the dorsum of the wrists in P5 at 12 years. (f) Wasting of thenar and hypothenar muscles of P10 at $10^{1}/_{2}$ years. (g) Woody skin on the dorsum of the wrists and fingers in P17 at 31 years. (h) Advanced wasting of the thenar and hypothenar muscles in P16 at 26 years.

The five patients from Turkey were first examined at a later age than patients in India. By that time, all of them had claw hand deformity, which manifested around the age of 10 years. Three of them had an initial diagnosis of rheumatoid arthritis and two had an erroneous diagnosis of scleroderma (Table 2).

Difficulty in squatting was experienced by 11 of 12 children; the youngest patient to present with this symptom was 5 years old (Fig. 2d). Genu valgum was observed in 13 of 18 patients, including all patients from India, except patient 1, and it progressed with advancing age (Fig. 2e). The kyphoscoliotic deformity in five adults from Turkey was similarly progressive. Worsening of hip pain and ensuing difficulty in walking was a major complication from adolescence in six of 18 patients. This is also a major complication in adolescents with ML-IIIαβ (Cathey *et al.*, 2010). In the present cohort, hip joint replacement was performed around the latter half of first and early second decade in two of 18 patients, but hip disease had not resulted in loss of ambulation or wheelchair confinement in anyone in this cohort of ML-IIIγ patients.

Imaging studies

Slowly progressive dysostosis multiplex (Spranger *et al.*, 2012) manifested as gradually worsening skeletal features in ML-IIIγ and the radiological features are not discernible from ML-IIIαβ. Delayed bone age was found consistently in all patients younger than the age of 18 years. The carpal bones had an irregular shape and were smaller than normal (13/18) (Fig. 3a). Proximally pointed metacarpals were a constant finding in the Indian cohort (Fig. 3b), but not in the Turkish adult patients (Fig. 3c). Oar-shaped ribs were observed in 14 of 18 patients as early as 5 years (Fig. 3d). Anterior–inferior beaking in one or more lower thoracic or upper lumbar vertebrae was apparent in 13 of 18 patients (Fig. 4a–c). Remarkably, this component of the radiographic phenotype was lacking in the patients from Turkey, except for its mild expression in patient 15 (Fig. 4d). Scoliosis was a late feature in five of eight adults (Fig. 3g), and was

Table 2 Investigations and previous diagnoses in 18 patients

Families	1	2		3	4	5	6		7		8		9		10		11	12
Patient number	1	2	3	4	5	6	7	8	9	10	11	12	13	14	15	16	17	18
Nerve conduction	CN	CN	CN	CN	CN	CN	CN	CN	CN	CN	ND	CN	CN	CN	CN	CN	CN	–
Plasma lysosomal enzymes (fold)																		
α-Mannosidase	61	59	57	110	29	–	5.8	4.1	5.1	3.8	ND	3	40	31	64	95	98	ND
β-Hexosaminidase (A and B)	3.4	2.6	3.6	3.4	2	6.6	1.9	5.4	7.8	2.5	ND	20	4.1	4.3	10.6	9.5	7.1	ND
β-Glucuronidase	–	–	18	29	24	19	ND	13	13.9	ND	ND	8	ND	ND	ND	ND	ND	ND
Previous diagnosis	RA	RA	MPS-IV	MPS-IV	RA	ML-III	ML-III	MPS	MPS	ML-II/ ML-III	ML-II/ ML-III	MPS-IV	RA	Scl	RA	Scl	RA	PPRD
Mutation	c.233 + 1 G > A	c.233 + 1 G > A	c.323 G > A	c.323 G > A	c.323 G > A	c.323 G > A	c.323 G > A	c.323 G > A	c.323 G > A	c.512 ins GTGG	c.512 ins GTGG	c.323 G > A	c.499 dupC	c.499 dupC	c.499 dupC	c.499 dupC	c.499 dupC	c.607 C > T

AS, aortic stenosis; AV, aortic valve; CN, compressive neuropathy; ML, mucolipidosis; MPS, mucopolysaccharidosis; MR, mitral regurgitation; MV, mitral valve; ND, not done; PPRD, progressive pseudorheumatoid dysplasia; PR, pulmonary regurgitation; RA, rheumatoid arthritis; Scl, scleroderma; TV, tricuspid valve.

present from childhood only in patient 8. Narrowing of the intervertebral spaces was consistent in all available radiographs of the adult MLIII γ patients (Fig. 3f and g). Sclerotic margins of upper and lower vertebral end plates were observed from childhood.

All 10 children had hypoplasia and narrowing of the lower ilia with slanting of the acetabular roof, a consistent feature also in patients with either ML-II or ML-IIIαβ (Fig. 5a–c). Six of eight adult patients also had tapering of the lower ilia. Narrowing of the hip joint was consistently evident from early adolescence (Fig. 5d). Proximal femoral epiphyseal irregularity or flattening concomitant with narrowing of the joint space and widening of the femoral neck was found in 16 of 18 patients, including a 5-year-old patient. Pain and restriction of hip joint movements because of severe destructive changes required bilateral surgical replacement of hip joints in two of 18 cases (patients 13 and 15); the earliest replacement was at the age of 18 years (Fig. 5e). Coxa valga ranging from 142° to 152° was evident in 13 of 18 patients (normal: 120°–135°) (Fig. 5a–d) and this warranted a bilateral subtrochanteric osteotomy for patient 14 at 16 years. Genu valgum was surgically corrected in one 12-year-old girl who had rapid progression (patient 5) (Fig. 3e).

Echocardiographic evaluation showed a thickened, myxomatous mitral valve in five of 11 patients and mild mitral regurgitation in five of 11 patients (Fig. 6). Patient 18 had mild aortic stenosis. Patient 1 had myxomatous thickening of both the tricuspid and the mitral valve with mild regurgitation of both the atrioventricular valves. Unfortunately, the adult Turkish patients underwent no echocardiographic evaluation.

Biochemical and molecular evaluation

The specific activities of α-D-mannosidase, β-D-hexosaminidase A and B and β-D-glucuronidase were assayed as representative lysosomal acid hydrolases in plasma. α-D-mannosidase was consistently elevated, ranging from 3- to 110-fold (15/15). β-D-Hexosaminidase activity was enhanced by 1.9–20-fold in all of 16 patients. β-D-Glucuronidase ranged 8–29-fold above the control values in all of seven studied patients (Table 2).

Five pathogenic *GNPTG* mutations, three of them novel, were identified. All patients had homozygous pathogenic variants and the parents were confirmed to be heterozygotes for the corresponding mutations. The three novel mutations were detected in the patients from India. The c.233 +1 G > A alteration found in two siblings disrupts a consensus splice site and is expected to result in aberrant exon 4 splicing. The novel variant c.323 G > A; p.W108X, a nonsense alteration in exon 6 of *GNPTG*, was identified in six unrelated families, all hailing from northern Kerala in India. A third novel mutation c.512insGTGG; p. H172Wfs*28 detected in exon 7 causes a shift of the

Fig. 2

(a) Restricted shoulder abduction in P2 at 13 years. (b) Hypertrophy of the forearm and supination defect with wasting of hypothenar muscles in P6 at 7 years. (c) Slit-lamp study in P1 showing corneal clouding that is homogenous in nature and stromal in location (white arrow). The slit beam shows clearly that the epithelium is uninvolved. (d) Bilateral contracture of the ankle leading to difficulty in squatting for P1 at 14 years; his hands show clawing and widening of the wrists. (e) Genu valgum in P5 at 12 years. (f,g) Coarse face of P3 and P10 at 10 years.

reading frame and premature truncation of the GNPTG polypeptide. This pathogenic variant was found in two siblings from Karnataka, India. One of the two previously reported *GNPTG* mutations, the c.499dupC frame shift variant was detected in all five Turkish patients from three unrelated families. The White patient was homozygous for the second known mutation: c.607 C > T; p. Asp171Glufs*19 (Table 2).

Discussion

The detailed description of the phenotype of the children in this cohort shed light on clinical differences between ML-IIIαβ and ML-IIIγ. The molecular confirmation of the clinical diagnosis of ML-IIIγ in a cohort of 18 patients mainly from India and Turkey is the result of fruitful international collaboration among clinical geneticists and molecular laboratories. The two nonallelic but similar clinical entities have hitherto been considered to be indistinguishable. The age of onset is usually between 3 and 5 years in both types of ML-III, except the later onset ML-IIIαβ patients with biallelic missense mutations. The later onset in the Turkish patients is most probably actually a result of later diagnosis because of the extreme rarity of ML-IIIγ and the close phenotypic similarity to rheumatoid arthritis. Defining the true age of clinical onset in any chronic inborn error of metabolism is truly challenging, and the later onset GNPT-related mucolipidoses are no exception.

The earliest symptom of stiffness and painful, limited range of motion in small joints in the hands and fingers, leading to clawing, is present in ML-IIIαβ by 3–5 years, but with less severity in ML-IIIγ. In a recent longitudinal study of 11 patients from Turkey with ML-IIIγ, stiffness of fingers was evident as early as 1.5 years (Tüysüz *et al.*, 2018). Nerve conduction velocity slowing has not consistently been measured in ML-IIIαβ as it has been in this study. Wasting of the thenar and hypothenar muscles was evident in our cohort as early as by 7–9 years. Early symptoms of carpal tunnel syndrome as well as the early

Fig. 3

(a) Radiograph of wrist of P5 at 5 years shows bone age corresponding to 3 years with proximal tapering of the metacarpals from 2 to 5 with irregular carpals. The position of the medially placed thumb is because of associated difficulty in supination. (b) Radiograph of hands of P5 at 12 years showing clawing of fingers with severe shortening of 3–5 metacarpals with proximal pointing and irregular carpals with ball and socket deformity of 2–5 metacarpals and ivory epiphysis for 2–5 terminal phalanges. (c) Hand radiograph at 26 years showing reduced space between carpals and a narrow joint space for metacarpophalangeal and interphalangeal joints. (d) Chest radiograph of P1 showing oar-shaped ribs. (e) Genu valgum in P3. (f) Very narrow intervertebral space in the thoracolumbar region in P11 at 20 years. (g) Severe scoliosis toward the right in P10 at 26 years and hips show bilateral prosthesis.

difficulty in squatting might not have received sufficient attention in the adult patients.

The poorly understood phenomena leading to progressive hardening of skin and connective tissue throughout the body in either condition may not have received adequate attention in the past. Woody skin was observed in 16 of 18 patients. It appears first on the dorsum of the hands and manifests later in the facial skin. The skin changes had led to a provisional diagnosis of sclerodema in patients 14 and 16. This feature has, to our knowledge, not been reported in the mutation confirmed reports on ML-IIIαβ. However, stiffness of shoulder joints, which is evident at birth in ML-II, and is an early finding in ML-IIIαβ patients, is not reported in ML-IIIγ before 6 years.

Apparent hypertrophy of the forearms, mostly at its radial side, was observed in seven of 18 patients, and was evident as early as 7 years. This feature has never been reported in ML-IIIαβ. Magnetic resonance fast spin-echo T2-weighted image of the hypertrophied forearm in patient 5 at the level of mid arm and upper forearm showed normal muscle bulk without infiltration or abnormal fat proliferation. Thus, the apparent hypertrophy might be because of the gradual replacement of muscle by soft connective tissue rather than muscular hypertrophy. The underlying reason for deficient supination needs further study.

Cardiac valve pathology, also an expression of slowly progressive hardening of connective tissue, shows remarkably variable clinical onset, and is a major concern as it may lead to fatal heart failure in the later stages of the disease process.

At variance with the poorly understood pathology in connective tissue, the skeletal aspects are well defined in both ML-IIIαβ and ML-IIIγ (Spranger *et al.*, 2012). Recognition of dysostosis multiplex in key radiographs in

Fig. 4

Radiograph of spine lateral view (a) minimal beaking of the lower thoracolumbar spine at 5 years. (b) Antero-inferior hooking of the lower spine (white arrow) at 10.5 years. (c) Very prominent anterior hooks in the upper lumbar vertebra at 14 years (white arrow) and posterior subluxation of S1 (black arrow). (d) Irregular upper and lower end plates of the lumbar vertebrae with narrowing of the intervertebral disc spaces with short pedicles at 26 years.

association with early clawing of fingers should clinch the diagnosis of chronic GNPT-related mucolipidoses.

Hip pathology is a hallmark of ML-IIIαβ and ML-IIIγ patients, and manifests in adolescence in both conditions. Severe pain and complete destruction of the hip joints have led to loss of ambulation and wheelchair confinement in many αβ patients; however, total hip replacement has been partially successful in both disorders. Cyclic intravenous treatment with bisphosphonates may postpone but not prevent the need for surgery. Tüysüz *et al.* (2018) used cyclic bisphosphonates for three patients with osteopenia and observed a reduction in bone pain and improvement in mobility. In our cohort, no patient has completely lost ambulation, although walking was often difficult and required bilateral hip replacements for patient 13 and patient 15 by the second decade. In the recently reported Turkish cohort, a 14-year-old boy underwent three corrective surgeries for coxa valga over a 7-year follow-up period (Tüysüz *et al.*, 2018).

Corneal clouding is a consistent feature in both ML-IIIαβ and ML-IIIγ. This can be detected by a simple, non-invasive, slit-lamp evaluation and was evident as early as $5^{8}/_{12}$ years of age in one patient with ML-IIIγ. The corneal clouding develops at a very early age as fine homogenous corneal opacities in the anterior and posterior stroma, progresses to involve the full corneal thickness, and spares the epithelium (Traboulsi and Maumenee, 1986) (Fig. 2c). The sparing of epithelium could partially explain the good prognosis for visual acuity as the interface between the cornea and the tear film remains normal and regular.

The molecular studies of this cohort confirm exclusively homozygous mutant genotypes in all patients. The culprit mutant genotypes in this cohort of ML-IIIγ and nearly all of the mutant genotypes reported previously were homozygous for 'severe-effect' or 'amorph' variant *GNPTG* alleles. All types of variants including splicing, insertions, deletions, missense, and nonsense mutations in *GNPTG* have been associated with ML-IIIγ, but

Fig. 5

Radiograph of pelvis anteroposterior view. (a) At 5 years showing tapering of the lower ilia with mild dysplasia of the upper femoral epiphysis. (b) Progression of dysplasia of the upper femoral epiphysis and tapering of the lower ilium with slanted acetabular roof at 7 years. (c) At 12 years shows severe flattening of the upper femoral epiphysis. (d) At 20 years showing narrowing of hip joints, an irregular acetabular margin with flattening of the upper femoral epiphysis. (e) At 26 years showing bilateral total hip replacement. In addition, figures (a)–(d) show coxa valga.

Fig. 6

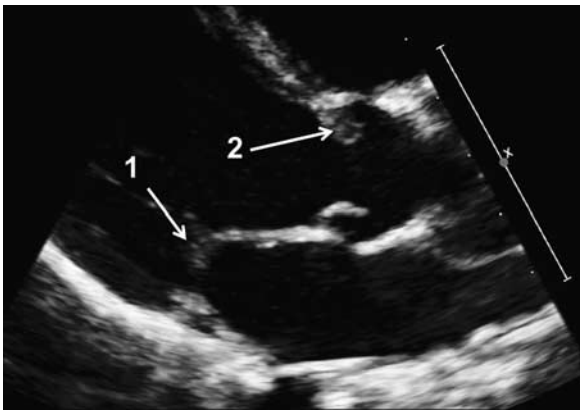

Echocardiographic image showing a parasternal long-axis (PLAX) view still-frame of P8 showing mild thickening of the anterior mitral valve leaflet (arrow 1) and the aortic valve leaflet (arrow 2).

homozygosity appears to be the rule rather than the exception (Velho *et al.*, 2016). The few missense mutations were interpreted as affecting highly conserved amino acids of catalytic importance in the γ-polypeptide (Persichetti *et al.*, 2009). The soluble GNPTG polypeptide normally binds to the Golgi membrane-bound nascent GNPTAB complex of proteins to play its minor role. The question arises whether homozygous or compound heterozygous missense mutant genotypes in *GNPTG* result in a barely recognizable or even a subclinical phenotype. Careful genotype–phenotype correlation is needed to identify the possible existence of an ML intermediate entity between ML-II and ML-IIIαβ (Cathey *et al.*, 2010; Leroy *et al.*, 2014; Qian *et al.*, 2015). Tüysüz *et al.* (2018) have confirmed that only mutations with 'severe effect' were identified in a cohort of Turkish ML-IIIγ patients. In contrast, in ML-IIIαβ patients, 'severe-effect' and 'mild-effect' mutant alleles are distributed more evenly. This is the probable explanation

for the apparently larger spectrum of clinical variability in ML-IIIαβ. Earlier reports on smaller patient cohorts (Raas-Rothschild *et al*., 2000, 2004; Raas-Rothschild and Spiegel, 1993–2016; Gao *et al*., 2011) have reported ML-IIIγ patients mainly from the Middle East and Mediterranean region and as the rarest of the delineated MLIII types. This report of ML III gamma, which is the rarest form of ML III, has cases from both India and Turkey, indicating that it is a pan-ethnic disorder rather than a purely regional disorder. This has also been shown by an Italian cohort (Persichetti *et al*., 2009). Not a single patient with ML-IIIαβ has been diagnosed within the time frame of 12 years from Kerala, the southern state of India, where the study was carried out. Meanwhile, several other rare autosomal recessive skeletal dysplasias and lysosomal storage disorders have been identified in this region, including 10 patients with ML-II (Nampoothiri *et al*., 2014). These findings suggest that ML-IIIγ is more frequent in the state of Kerala than ML-IIIαβ. In our cohort, parental consanguinity has been confirmed in eight of 12 families. The c.323 G > A/p.W108X nonsense variant found in six unrelated families all hailing from northern Kerala points to the probability of a founder mutation as the most likely explanation.

Conclusion

The major clinical differences noted between ML-IIIαβ and ML-IIIγ, such as the hitherto unreported features of hypertrophy of forearms and supination defect, need to be studied prospectively in larger groups of patients recruited by international cooperation to provide a more definite answer to the question of clinically distinguishing ML-IIIαβ and ML-IIIγ. Obviously, any clinical difference cannot substitute for the diagnostic power of the gene mutation screening tests, but when supported by molecular confirmation, these may contribute toward more insight into the pathogenesis of ML. The results of the current study have provided an interesting base for such future studies.

Acknowledgements

The authors thank the families from three different countries for cooperating in this study. They declare that the authors have contributed to, read, and approved the final manuscript.

Conflicts of interest

There are no conflicts of interest.

References

Cathey SS, Leroy JG, Wood T, Eaves K, Simensen RJ, Kudo M, *et al.* (2010). Phenotype and genotype in mucolipidoses II and III alpha/beta: a study of 61 probands. *J Med Genet* **47**:38–48.

Encarnação M, Lacerda L, Costa R, Prata MJ, Coutinho MF, Ribeiro H, *et al.* (2009). Molecular analysis of the GNPTAB and GNPTG genes in 13 patients with mucolipidosis type II or type III: identification of eight novel mutations. *Clin Genet* **76**:76–84.

Gao Y, Yang K, Xu S, Wang C, Liu J, Zhang Z, *et al.* (2011). Identification of compound heterozygous mutations in GNPTG in three siblings of a Chinese family with mucolipidosis type III gamma. *Mol Genet Metab* **102**:107–109.

Hasilik A, Von Figura K (1981). Oligosaccharides in lysosomal enzymes. Distribution of high-mannose and complex oligosaccharides in cathepsin D and beta-hexosaminidase. *Eur J Biochem* **121**:125–129.

Hasilik A, Von Figura K (1986). Lysosomal enzymes and their receptors. *Annu Rev Biochem* **55**:167–193.

Kornfeld S (1992). Structure and function of the mannose 6-phosphate/insulinlike growth factor II receptors. *Annu Rev Biochem* **61**:307–330.

Kudo M, Brem MS, Canfield WM (2006). Mucolipidosis II (I-cell disease) and mucolipidosis IIIA (classical pseudo-hurler polydystrophy) are caused by mutations in the GlcNAc-phosphotransferase alpha/beta-subunits precursor gene. *Am J Hum Genet* **78**:451–463.

Leroy JG (2011). I-Cells and I-cell disease: text accompanying photograph. *Am J Human Genet* **89**.

Leroy JG, DeMars RI, Opitz JM (1969). I-cell disease. *Birth Defects Orig Art Ser* **4**:174–185.

Leroy JG, Sillence D, Wood T, Barnes J, Lebel RR, Friez MJ, *et al.* (2014). A novel intermediate mucolipidosis II/IIIαβ caused by GNPTAB mutation in the cytosolic N-terminal domain. *Eur J Hum Genet* **22**:594–601.

Marschner K, Kollmann K, Schweizer M, Braulke T, Pohl S (2011). A key enzyme in the biogenesis of lysosomes is a protease that regulates cholesterol metabolism. *Science* **333**:87–90.

Nampoothiri S, Yesodharan D, Sainulabdin G, Narayanan D, Padmanabhan L, Girisha KM, *et al.* (2014). Eight years experience from a skeletal dysplasia referral center in a tertiary hospital in Southern India: a model for the diagnosis and treatment of rare diseases in a developing country. *Am J Med Genet Part A* **164**:2317–2323.

Persichetti E, Chuzhanova NA, Dardis A, Tappino B, Pohl S, Thomas NS, *et al.* (2009). Identification and molecular characterization of six novel mutations in the UDP-N-acetylglucosamine-1-phosphotransferase gamma subunit (GNPTG) gene in patients with mucolipidosis III gamma. *Hum Mutat* **30**:978–984.

Pohl S, Encarnacão M, Castrichini M, Müller-Loennies S, Muschol N, Braulke T (2010). Loss of N-acetylglucosamine-1-phosphotransferase gamma subunit due to intronic mutation in GNPTG causes mucolipidosis type III gamma: implications for molecular and cellular diagnostics. *Am J Med Genet A* **152A**:124–132.

Qian Y, Van Meel E, Flanagan-Steet H, Yox A, Steet R, Kornfeld S (2015). Analysis of mucolipidosis II/III GNPTAB missense mutations identifies domains of UDP-GlcNAc: lysosomal enzyme GlcNAc-1-phosphotransferase involved in catalytic function and lysosomal enzyme recognition. *J Biol Chem* **290**:3045–3056.

Raas-Rothschild A, Spiegel R (1993–2016). Mucolipidosis III gamma. In: Adam MP, Ardinger HH, Pagon RA, Wallace SE, Bean LJH, Stephens K, *et al*., editors. *GeneReviews®*. Seattle, WA: University of Washington.

Raas-Rothschild A, Cormier-Daire V, Bao M, Genin E, Salomon R, Brewer K, *et al.* (2000). Molecular basis of variant pseudo-hurler polydystrophy (mucolipidosis IIIC). *J Clin Invest* **105**:673–681.

Raas-Rothschild A, Bargal R, Goldman O, Ben-Asher E, Groener JE, Toutain A, *et al.* (2004). Genomic organisation of the UDP-N-acetylglucosamine-1-phosphotransferase gamma subunit (GNPTAG) and its mutations in mucolipidosis III. *J Med Genet* **41**:52.

Reitman ML, Kornfeld S (1981). Lysosomal enzyme targeting. N-Acetylglucosaminyl-phosphotransferase selectively phosphorylates native lysosomal enzymes. *J Biol Chem* **256**:11977–11980.

Saul RA, Proud V, Taylor HA, Leroy JG, Spranger J (2005). Prenatal mucolipidosis type II (I-cell disease) can present as Pacman dysplasia. *Am J Med Genet A* **135**:328–332.

Spranger JW, Brill PW, Nishimura G, Superti-Furga A, Unger S (2012). *Bone dysplasias: an atlas of genetic disorders of skeletal development*, 3rd ed. Oxford: Oxford University Press. pp. 601–604.

Taylor HA, Thomas GH, Miller CS, Kelly TE, Siggers D (1973). Mucolipidosis 3 (pseudo-Hurler polydystrophy): cytological and ultrastructural observations in cultured fibroblast cells. *Clin Genet* **4**:388–397.

Traboulsi EI, Maumenee IH (1986). Ophthalmologic findings in mucolipidosis III (pseudo-Hurler polydystrophy). *Am J Ophthalmol* **102**:592–597.

Tüysüz B, Kasapçopur Ö, Alkaya DU, Şahin S, Sözeri B, Yeşil G (2018). Mucolipidosis type III gamma: three novel mutation and genotype–phenotype study in eleven patients. *Gene* **642**:398–407.

Velho RV, Ludwig NF, Alegra T, Sperb-Ludwig F, Guarany NR, Matte U, *et al.* (2016). Enigmatic in vivo GlcNAc-1-phosphotransferase (GNPTG) transcript correction to wild type in two mucolipidosis III gamma siblings homozygous for nonsense mutations. *J Hum Genet* **61**:555–560.